Direct spectral distribution characterisation using the Average Photon Energy for improved photovoltaic performance modelling

Rajiv Daxini *, Yanyi Sun, Robin Wilson, Yupeng Wu *

Faculty of Engineering, University of Nottingham, Nottingham, NG7 2RD, UK

ARTICLE INFO

ABSTRACT

Accurate photovoltaic (PV) performance modelling is crucial for increasing the penetration of PV energy into the grid, analysing returns on investment, and optimising system design prior to investment and construction. Performance models usually correct an output value known at reference conditions for the effects of environmental and system variables at arbitrary conditions. Traditional approaches to correct for the effect of the solar spectrum on performance are based on proxy variables that represent spectral influences, such as absolute air mass (AM_a) and clearness index (K_t). A new methodology to account for the spectral influence on PV performance is proposed in this study. The proposed methodology is used to derive a novel spectral correction function based on the average energy of photons contained within the measured solar spectral distribution. The Average Photon Energy (APE) parameter contains information on the combined effects of multiple proxy variables and is not limited by climatic conditions such as cloud cover, as is the case with most traditional models. The APE parameter is shown to be capable of explaining almost 90% of the variability in PV spectral efficiency, compared to around 65% for AM_a. The derived APE function is validated and shown to offer an increase of 30% in predictive accuracy for the spectral efficiency compared with the traditional AM_a function, and a 17% improvement relative to the AM_a-K_t function.

1. Introduction

Since the first mass production of photovoltaic (PV) modules began in the 2000s [1], PV technology has been moving to the forefront of endeavours to mitigate climate change. The success of a PV system relies not only on the technical capacity of the system itself, but the accurate prediction of the system's performance under a certain set of technical and environmental conditions [2–4]. This forecasting practice is known as Photovoltaic Performance Modelling (PVPM).

Predicting PV power output under real weather conditions is essential for PV system designers, investors and policy makers, energy suppliers, and end-users [5]. For example, performance predictions can be used to calculate financial savings for the end user, optimise system design prior to investment and construction, and facilitate greater PV grid penetration by providing timely performance predictions so energy from different sources can be balanced for a reliable and efficient supply [6,7].

The availability of solar irradiance is one of the most obvious considerations in PVPM [8–10], but the spectral distribution of the available irradiance is a more subtle yet also critical parameter that must be considered when evaluating how a PV system will perform [11–13].

Neglecting the spectrum can lead to significant errors in PV performance forecasts. The magnitude of these errors is strongly correlated with the type of PV technology under investigation since the spectral response (SR) of a PV device is determined by the cell construction and semiconductor material.

In terms of semiconductor material, for example, amorphous silicon (aSi) technologies have a particularly wide band gap, and therefore narrow SR. Under realistic operating conditions (ROCs), the fraction of the spectrum that lies within the useful range of aSi modules can vary by +10% to −15% with respect to standard test conditions, which translates into deviations in performance of up to 20% [14–16]. In terms of cell construction, a higher level of sensitivity to spectral variations has also been found for double junction technologies [17], such as GaAs/Ge devices. On the other hand, the output from some PV technologies, such as multi-crystalline-Si, is not particularly sensitive to the spectral distribution of incident solar radiation [18].

The significant and varied impact of the spectrum on PV output, dependent on the interplay of multiple factors, lays bare the complexity of modelling such effects and hence the need for comprehensive spectral correction functions. There exist many approaches to modelling the spectral influences on PV output. One of the first models developed, still

---

* Corresponding authors.
E-mail addresses: Rajiv.Daxini@nottingham.ac.uk (R. Daxini), Yupeng.Wu@nottingham.ac.uk (Y. Wu).

in use today, is the absolute air mass function $f(\text{AM}_a)$ [19], which uses AM_a as a proxy for the spectral influences on I_{sc}. However, $f(\text{AM}_a)$ is defined only for clear skies, consequently rendering it unsuitable for regions where cloud cover is the norm, such as northern and central Europe. In such locations, it is estimated that 50% of the time there may be cloud cover, which has a significant impact on spectrum resulting in higher levels of scattering and thus a shift to bluer spectra [20]. An extensive study based on spectral and PV performance measurements from multiple sites in Japan [21] corroborates the findings in Ref. [20] of the impact of cloud cover on the spectrum. The subsequent impact of cloud-induced spectral changes on PV performance are also found to be especially significant for particular PV technologies, such as hydrogenated aSi modules, for which fluctuations in performance of $\pm 10\%$ were observed [21]. Other studies have also affirmed the importance of clouds on the spectrum, and hence the output of aSi [14] and c-Si [22] devices in particular.

In addition to cloud cover, there are many other factors unaccounted for by $f(\text{AM}_a)$ that have a non-negligible effect on the spectrum of solar irradiance, such as turbidities, ozone, and the variable presence of other atmospheric gases such as water vapour and SO_2 [20,23–25]. It is emphasised by Klise et al. (2015) in particular that these atmospheric components, in particular atmospheric water vapour and turbidities, can impact the spectrum even in clear sky conditions [26]. The unequivocal dependence of the spectrum on factors other than air mass, present in both clear and non-clear-sky conditions, means that the overall effect of the spectrum on PV output is underestimated by the AM_a spectral correction function. It is important to note that although in certain clear sky conditions the air mass may be representative of the majority of spectral influences on I_{sc} [19], research has shown that even in these conditions $f(\text{AM}_a)$ carries with it uncertainties. For example, Klise et al. (2015) find a systematic error in the air mass function where, at the same air mass, the spectral effects on I_{sc} vary depending on the time of day [26].

Nelson et al. (2012) established an alternative spectral correction function using the atmospheric precipitable water content, W, instead of AM_a [27]. The model is derived for Cadmium Telluride (CdTe) PV technologies and validated in four climate regions. In an attempt to improve this model and expand its applicability to multiple technologies, Lee and Panchula (2016) proposed a spectral correction surface function based on both AM_a and W, which they validate for both CdTe and c-Si PV technologies [28]. Duck and Fell (2016) build on Ref. [28] by investigating the applicability of the surface function to additional locations, and refining model predictions through the use of additional parameters [29]. However, these studies rely on spectral distributions simulated using the SMARTS model, which is a clear sky spectral irradiance model [30]. Therefore, the application of these functions to cloudy sky conditions is limited.

The literature on spectral correction functions for cloudy conditions is sparse. Gottschalg et al. (2004) incorporated the effects of clouds into spectral correction work modelling by correlating AM_a and clearness index, K_t, with the Useful Fraction, UF [14]. The UF is an indicator of the amount of available solar irradiance that falls within the spectral response window of a particular PV device. A strong dependence of the UF on air mass and the clearness index is shown, thus affirming the significance of cloud-induced spectral shifts on PV performance. Duck and Fell (2015) include the AM_a-K_t function in a review of different spectral correction functions [31]. In this review, it was found that the AM_a-K_t model offers advantages over the traditional AM_a model, but could be improved further when a weighted Useful Fraction (WUF) is used in place of the useful fraction (UF). Whereas the UF assumes a constant spectral response within the useful range of spectral irradiance, the WUF accounts for the non-constant PV spectral response over the range of wavelengths that fall into the useful range for a particular PV device [22].

Despite the improvements offered by the multivariable functions over the single variable approaches, these methods are still limited.

One reason is the inherent complexity of modelling and parameterising 3D surfaces. Another reason is the potential lack of generalisability of such functions in environments where the relative dominance of the influences of different atmospheric or meteorological parameters on different PV technologies or on the spectrum in different locations may vary. Therefore, the ideal solution would be a spectral correction function with as few values as possible containing the maximum amount of information on the dominant factors affecting the spectrum, whatever they may be.

One such candidate parameter is the Average Photon Energy (APE). The APE provides a direct quantitative characterisation of the final spectral distribution once it has already been influenced by all of the relevant environmental parameters in the region under investigation, whether it be air mass, clouds, precipitable water content, or anything else. This is in contrast to the traditional approaches that take one or two factors that can influence the spectrum and then use them as proxies for the total spectral influence on PV output. By definition, the APE should contain information on all parameters affecting the spectrum as it is a numerical representation of a measured spectral distribution after the photons in that distribution have already been affected by all environmental phenomena.

Parameters derived from the measured spectral distribution, such as APE, are being used more in recent years [32,33] as outdoor spectrometer devices are becoming more widely available, in particular due to technological developments leading to decreasing costs [34,35]. The APE in particular has been used extensively to characterise spectral irradiance distributions [36–40] and has been shown to be correlated with other spectral characterisation parameters such as the Useful Fraction (UF) [41]. However, the APE possesses certain advantages over other indicators. For example, unlike the UF, the APE is device independent. Another advantage of the APE, compared to AM_a for example, is that it can represent spectral conditions in both clear and cloudy skies.

It is argued in the literature that the APE is a single value that contains information on the dominant environmental conditions influencing PV performance and is therefore capable of effectively characterising the shape of the incident irradiance spectrum [18,42–44]. However, from a theoretical standpoint, two different spectra could have the same APE. This is possible since a decrease in one area of a spectral distribution could be compensated by an increase in another area, leading to the same average photon energy but a different shape of the overall spectrum. This potential lack of bijectivity is important because, if the APE parameter cannot reliably and uniquely characterise spectra over a suitable wavelength range for PV performance analysis, its applicability in such analysis would be severely restricted. By adopting the IEC's methodology for rating the spectral matching of a solar simulator [45], Minemoto et al. (2009) show that an APE value yields a spectral irradiance distribution with a relatively small standard deviation [46]. They conclude that the APE is in fact a bijective index that can uniquely represent different solar spectral distributions.

The relationship between the APE parameter and PV performance has been discussed in the existing literature. Cornaro and Andreotti (2013) present a detailed characterisation of their test site using the APE, but the data sample used for PV analysis spans only two summer months — June and July — thus restricting the applicability of the findings to other times of the year [36]. A similar limitation is faced by the work of Williams et al. (2003), which only presents results for the winter months [43]. Other work has shown the strong correlation between the APE and various PV (spectral) performance indicators, and thus the benefit of using the APE parameter to understand PV spectral efficiency [47–49]. However, these studies are limited in terms of their extension to a predictive model of PV performance based on spectral effects, and associated model validation.

In summary, existing spectral correction functions are based on proxy variables and suffer from various limitations, the most significant of which is their inability to model spectral influences accurately in
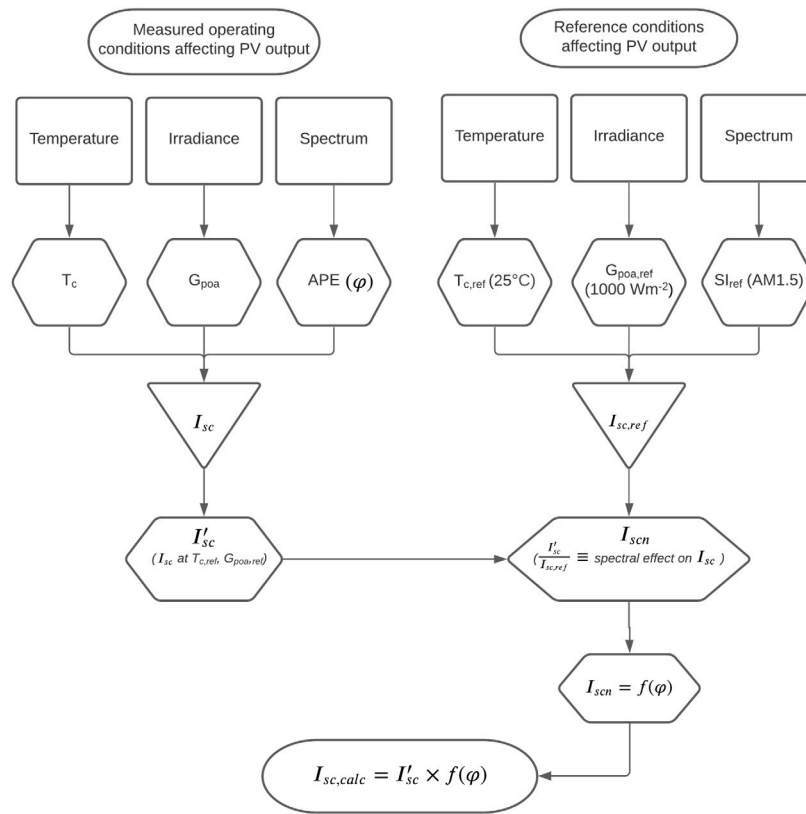
Fig. 1. Outline of the methodology to account for the spectral influence on PV performance using the APE parameter.

situations where the relative influences of different parameters on the spectrum may vary. Several studies have attempted to use measurements of the spectral distribution to understand the spectral effects on PV performance, in particular through use of the APE parameter. However, these studies are often limited in terms of data sample size, extension to a predictive model, and model validation.

This project proposes a new methodology by which the spectral influence on PV performance can be analysed. The proposed methodology is demonstrated using 12 months of outdoor performance data for an aSi PV module as an example. The derived spectral correction function, based on the APE parameter, is validated in all sky conditions and its performance is compared to that of two commonly used spectral correction methods. The coefficients of the derived spectral correction function are presented in this study so that the function may easily be integrated into any PV performance model in order to achieve improved PV performance forecasts.

2. Methodology

In this section, the key parameters underpinning the analysis of the study are introduced and explained, along with a description of the experiment campaign. The methodology used to develop and validate the proposed spectral correction function is also described and justified. Finally, a summary of the uncertainty analysis is presented.

The steps to derive the APE spectral correction function are summarised in Fig. 1. In the proposed methodology, the PV module short-circuit current measured at arbitrary conditions (I_{sc}), characterised by temperature, irradiance, and spectrum, is translated to a reference temperature and irradiance. This temperature– and irradiance-normalised short-circuit current, I'_{sc}, is compared to the short-circuit current measured at a reference temperature, irradiance, and spectrum, I_{sc0}. The ratio of the two currents indicates the spectral influence on I'_{sc}, which this study models using the APE parameter to derive a correction function that can easily be integrated into any PV performance model.

2.1. Characterisation of the spectrum

The Average Photon Energy parameter is adopted in this study as a means of characterising solar spectral distributions. The APE originates from considering the fundamental change in the physical nature of the photons when a spectral distribution is altered. Such alterations manifest themselves in shifts in the photon wavelength.

The wavelength of light (λ) is inversely proportional to its energy (E), where the constant of proportionality is the product of the speed of light in a vacuum (c) and Planck's constant (h):

$$E = \frac{hc}{\lambda}. \tag{1}$$

Therefore, if one considers the average energy of all of the photons in one spectral distribution, this value will provide an indication of the shape of the spectrum. The average energy of the photons in a spectral distribution is calculated by dividing the total energy in a spectrum by the total number of photons it contains [41]:

$$\text{APE [eV]} = \frac{1}{q} \left(\frac{\int_a^b E_\lambda d\lambda}{\int_a^b \Phi_\lambda d_\lambda} \right). \tag{2}$$

Here, $E(\lambda)$ [W m^{-2} nm^{-1}] is the spectral irradiance, $\Phi(\lambda)$ [m^{-2} nm^{-1}] is the spectral photon flux density, q [C] is the electron charge, and a [nm] and b [nm] are the upper and lower wavelength limits, respectively, of the considered waveband.

2.2. Characterisation of spectral effects on PV performance

The parameter used in this paper to quantify the effects of the spectrum on PV performance is the normalised short-circuit current, I_{scn}, which is calculated from the measured short-circuit current, I_{sc}.

In order to determine the purely spectral influence on I_{sc}, it is necessary to isolate the effects of other factors, namely irradiance and temperature. I_{sc} measured at different irradiances and temperatures
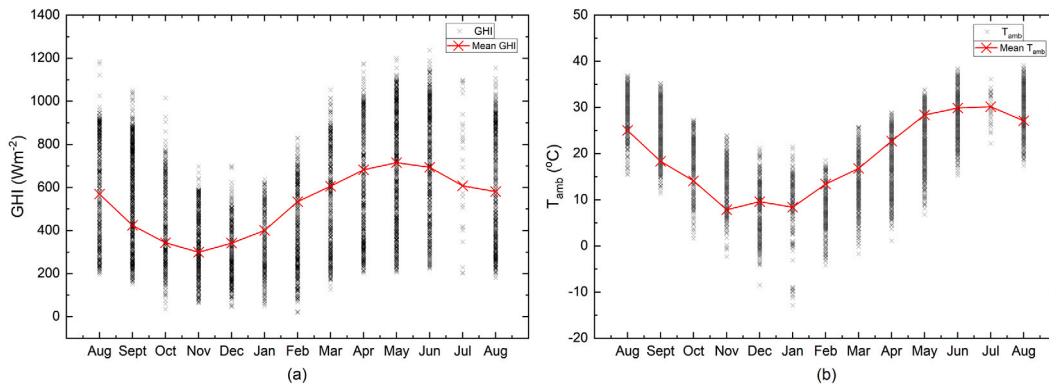
Fig. 2. Annual climatic conditions at the Golden test site. Panels (a) and (b) show the annual variation in the Global Horizontal Irradiance (GHI) and the ambient air temperature (T_{amb}), respectively.

can be translated to a reference temperature ($T_r = 25°C$) and reference irradiance ($G_0 = 1000$ W m^{-2}) [50]:

$$I'_{sc} = \frac{I_{sc}}{1 + \hat{\alpha}_{I_{sc}}(T_c - T_r)} \left[\frac{G_0}{G_{poa}} \right], \tag{3}$$

where $\hat{\alpha}_{I_{sc}}$ [°C^{-1}] is the short-circuit current temperature coefficient, T_c [°C] is the cell temperature, and G_{poa} [W m^{-2}] is the measured plane of array irradiance. T_c can be estimated using a one-dimensional thermal conduction model based on the module back surface temperature, T_m, which is measured:

$$T_c = T_m + \frac{G_{poa}}{G_0} \Delta T, \tag{4}$$

where ΔT is the temperature difference between the module and cell, which, based on the construction of the PV device analysed, is set as 3°C in this study [51].

The normalised short-circuit current, I_{scn}, is then found by dividing I'_{sc} by the reference short-circuit current, I_{sc0}, which is the current measured at the reference test conditions (T_r and G_0):

$$I_{scn} = \frac{I'_{sc}}{I_{sc0}}. \tag{5}$$

It is proposed in this work that the normalised current may be expressed as a function of the average photon energy, such that $I_{scn} = f(\varphi)$, where $f(\varphi)$ is a spectral correction function, dependent on APE, which models the spectral influence on I'_{sc} to explain the deviation of I'_{sc} from I_{sc0}. The proposed functional form of $f(\varphi)$ is a fourth order polynomial, with coefficients a_n, so in summary:

$$I_{scn} = f(\varphi) = \sum_{n=0}^{4} a_n \cdot \varphi^n. \tag{6}$$

The fourth order was determined to be optimal by testing functions of different forms. Increasing the order of the polynomial was found to improve the coefficient of determination for the fit, but beyond the fourth order these improvements were negligible relative to the precision with which the values of APE and I_{scn} are known.

The I_{scn} ratio in Eq. (5) is also helpful for understanding how a PV module responds to different spectral conditions. $I_{scn} > 1$ indicates higher performance under the prevailing spectrum with respect to the performance under the reference conditions, $I_{scn} < 1$ indicates decreased performance, while $I_{scn} = 1$ indicates there is no difference between the performance under the prevailing spectrum and under reference conditions.

2.3. Data sourcing and processing

The model development and validation are both based on data from two publicly available datasets from the National Renewable Energy

Laboratory (NREL). The PV performance and meteorological (PVM) data are sourced from the NREL Outdoor Test Facility [52], while the spectral irradiance (SI) data are sourced from the Measurement Instrumentation Data Centre at NREL [53]. The PV module used to validate the proposed model is an amorphous silicon device (NREL database ID 0308). Despite exhibiting a waning mainstream market share compared to crystalline silicon devices, aSi silicon devices are particularly relevant for applications with a large future growth potential such as building integrated photovoltaics [54–56]. The module characteristics, including the Sandia Model coefficients for the module, are provided in the NREL PVM dataset. The Golden (Colorado) site is the only site for which concurrent SI and PVM data were measured at the same location, hence only data from this site are used.

To illustrate the climatic conditions present at the test site, the annual variation in irradiance and ambient air temperature are presented in Fig. 2. The temperature and irradiance both follow the same trend throughout the year, and are indicative of a hot-summer and cold-winter environment.

A representative sample of SI and PVM data are required to derive the spectral correction function, which then must be capable of accurately modelling spectral effects for an arbitrary set of data. An investigation of the annual variation of APE at the Golden site is conducted to determine the number of months of data required to represent the full range of APE values possible in a typical year.

The annual variation of APE at the Golden site from August 2012 to August 2013 site is presented in Fig. 3. There is greater variability in APE from around November to February, which is likely to be a result of more unstable weather conditions that are typical in the winter. In addition, there is a dip in the average APE values for the winter months compared to the summer. This distinct seasonal variation in the APE from summer to winter is likely to be driven primarily by the lower position of the sun in the sky in winter, and hence higher air mass.

Based on this annual variation in APE, a sample from January 2013 to August 2013 is used to provide a suitable range of spectral data for the model development, that is one which includes the full range of possible annual APE values, while the remainder is used for the model validation. The validation dataset also includes the full range of possible values, although the overall size of the sample is smaller. In Section 3, the fit statistics for the model developed on the model development data are cross-checked against the same fit for the full one-year dataset to test the reliability of the model development data.

The APE values in Fig. 3 are all calculated from the spectral irradiance (SI) data measured using an EKO MS-700 Global spectrometer facing south, at a tilt of 40°, which corresponds to tilt and orientation of the PV module under investigation. The SI data have a one-minute resolution between the hours of approximately 0600h and 1800h, while the PVM data have a fifteen-minute resolution between similar hours. A subset of these data between the hours of 0800h and 1600h was
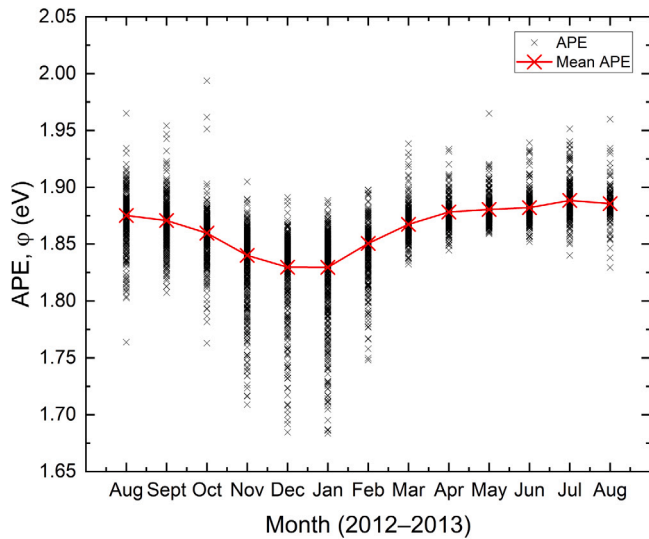
Fig. 3. Annual variation in APE for August 2012 to August 2013.

Table 1
Polynomial coefficients for the APE spectral correction function derived from January 2013–August 2013 data (Fig. 5, Eq. (6)).

	a_0	a_1	a_2	a_3	a_4
Value	−2500	5552	−4626	1715	−238

extracted to ensure a focus on daylight hours only. In total, around 200,000 spectral distributions and 11,000 PVM measurements were obtained. Measurements obtained under conditions with less than 200 W m^{-2} were omitted to reduce noise whilst still retaining measurements made in heavily overcast conditions [21,22]. Some measurements were missing from both datasets due to external factors such as instrument downtime. Therefore, only measurements of one parameter for which there existed a concurrent measurement of all other required parameters were retained. After processing, a final dataset of approximately 6300 measurements of each parameter was used.

2.4. Uncertainty analysis and fitting procedure

The methodology for determining the uncertainties on all of the measured parameters is explained in detail in Appendix B of the database's associated user's manual [52]. In this study, the provided uncertainty values are propagated through to the calculated variables using a simple calculus-based approximation [57]. The final error bars generated are used to apply an instrumental weighting to each data point in the fitting procedure for all graphs. For the non-linear curve fits, the Levenberg–Marquardt iteration algorithm is used.

3. Derivation of the APE spectral model

The analysis in Section 2.3 defines the model development and validation datasets as January–August 2013 and August–December 2012, respectively, based on the goal of including in each dataset the full range of possible PVM and SI values. As a secondary check of the representability of the model development data, the model derived from these data is compared to one derived from a full year of data.

The correlation between the APE and normalised short-circuit current, I_{scn}, for August 2012–August 2013 is presented in Fig. 4. Several parameterisations were tested and the optimal form was found to be a fourth order polynomial function, as described in Eq. (6).

The same correlation is presented for the sub-sample of data between January and August of 2013 in Fig. 5. The R-square coefficient of determination (R^2) for the proposed spectral function derived from the January–August data is 0.870. This value of R^2 is close to that of the function derived from the full year of data, 0.886, indicating a high similarity between the sub-sample and the full sample. For comparison, the same order polynomial plotted for September 2012–February 2013 yielded an R^2 value of 0.925, which suggests that this sample is not

representative of the overall population data (the full-year dataset), which may be a result of over fitting.

From considering the annual range of APE values, as done in Section 2 and this comparison of R^2 values, it may be concluded that the January–August sub-sample is representative of a typical annual dataset and may therefore be used to derive a general model for forecasting at any point during the year.

For the January–August sample plotted in Fig. 5, there is still a high goodness of fit of $f(\varphi)$ to the data, with almost 90% ($R^2 = 0.886$)of the variability in I_{scn} being described by the dependent variable, APE. The majority of the uncertainty in the fit appears to be around the 1.88 eV–1.90 eV where there is a higher variability in I_{scn} for the same APE values. Beyond 1.88 eV, the trajectory of increase in I_{scn} changes as I_{scn} plateaus off. This plateau may be a result of the limited spectral response range of the aSi module. The coefficients for the January–August 2013 model are presented in Table 1.

4. Model validation and discussion

The proposed model is validated using new data from August–December 2012. The normalised measured current from this period, hereinafter denoted "measured current" ($I_{scn,meas}$) for simplicity, is compared to the normalised current calculated using the proposed $f(\varphi)$ model, denoted $I_{scn,\varphi}$. In addition, the prediction accuracy of $f(\varphi)$ is compared to that of the absolute air mass function, $f(AM_a)$, which is the traditional spectral correction approach used in the Sandia Array Performance Model [51]. A comparison is also made with a modified version of the AM_a function, originally published in [14], which adds the spectral effects of cloud cover into $f(AM_a)$ by means of the clearness index, K_t.

The predictive accuracy is analysed in two ways. One is by directly comparing the predicted values with the measured values to analyse the error in the prediction at different APE ranges. Another involves plotting the data as a time series to identify any temporal phenomena underlying the deviations between the measured and predicted values, and to evaluate the temporal resolution at which accurate predictions of I_{scn} are possible.

4.1. Predictive accuracy of the APE spectral correction

Fig. 6 shows the predicted and measured normalised current values as a function of time, for the period from August to December 2012. The predicted values are calculated by substituting only the APE values for this period into the model presented in Fig. 5. There is a high degree of matching between the predicted and measured values of PV performance, both for values of I_{scn} greater than and less than unity, throughout the year. There appear to be two main types of temporal fluctuations in the data. One is the high frequency (15-min) fluctuations happening throughout each day, while another is the overall drop in $I_{scn,meas}$ as the seasons progress from summer to winter. The APE function is able to forecast accurately both the high frequency (15-min) fluctuations and the long-term seasonal shift in PV performance.

Fig. 7 presents the correlation between $I_{scn,meas}$ and $I_{scn,\varphi}$. The regression in Fig. 7 indicates that $f(\varphi)$ is an accurate and reliable predictor of I_{scn}. Firstly, the Pearson's r value of 0.969 indicates a very strong positive relation between the predicted and measured values of I_{scn}. Secondly, the R^2 of 0.940 substantiates the positive correlation between the two, and affirms the high degree to which the modelled current matches the measured current. As a measure of the variability
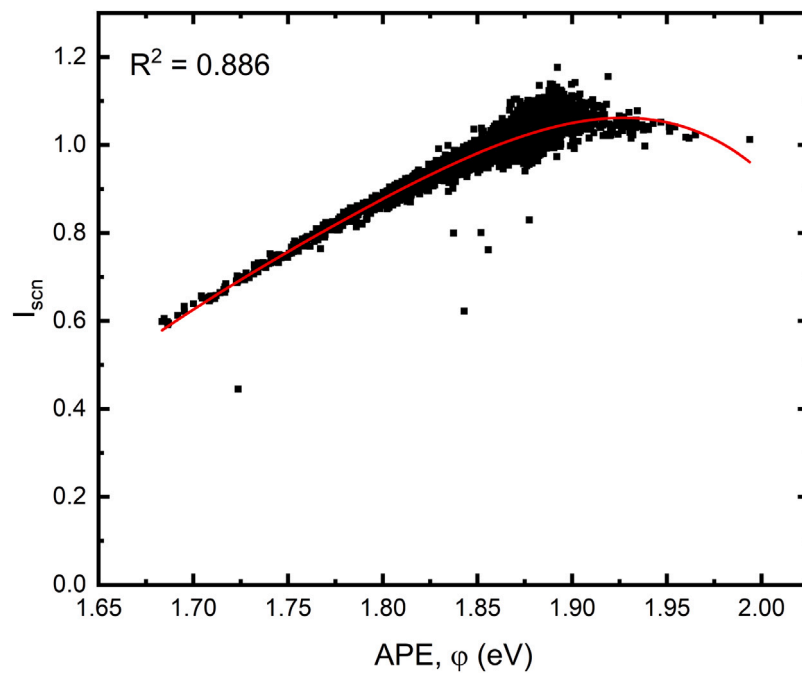
Fig. 4. Fourth order polynomial APE spectral correction function based on one year of data from August 2012 to August 2013 measured at Golden, Colorado.
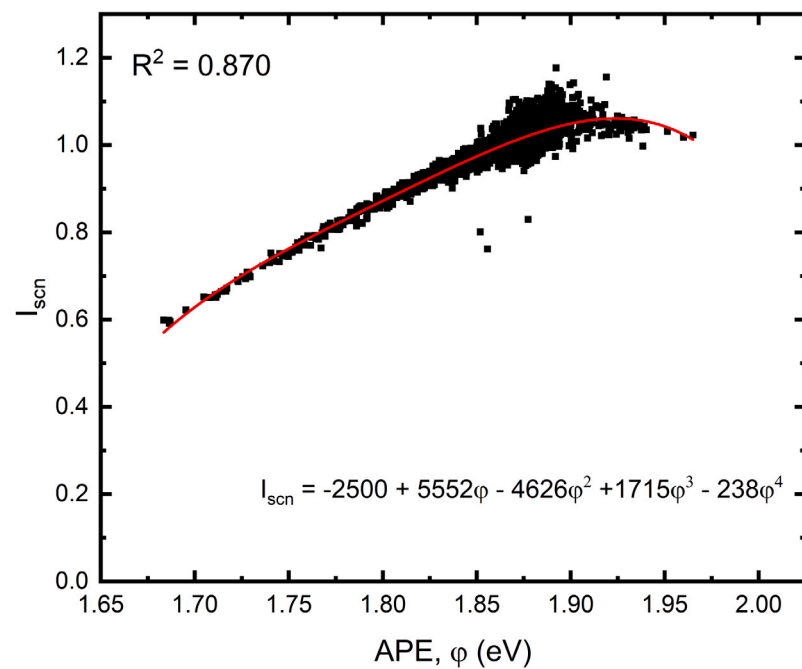

Fig. 5. Fourth order polynomial APE spectral correction function based on data from January 2013 to August 2013 measured at Golden, Colorado.

between the measured values and those predicted by the proposed model, the Mean Absolute Error (MAE) is found to be only 0.014, which indicates a high degree of matching between the measured and predicted values. Finally, the regression equation in Fig. 7 also indicates a low random and systematic error present in the data.

There appears to be a slight drift in the data away from the line of best fit in Fig. 7 at I_{scn} values less than 0.65. This drift may be a result of less data in the low APE value range used to derive the model. When comparing the data subset (Fig. 5) with the annual dataset (Fig. 4), in the data subset there are less data at low APE values in particular. The reduction may not only be responsible for the slightly lower R^2 value

for the subset $f(\varphi)$ fit, but also increased uncertainty and therefore more likely natural fluctuation in the spread of data in Fig. 7 at lower APE values.

4.2. Comparison with existing functions

This section of the analysis compares the predictive accuracy of the derived APE function to that of two existing functions from the literature. The same methods of analysis are used — absolute predictive accuracy test and time series analysis.
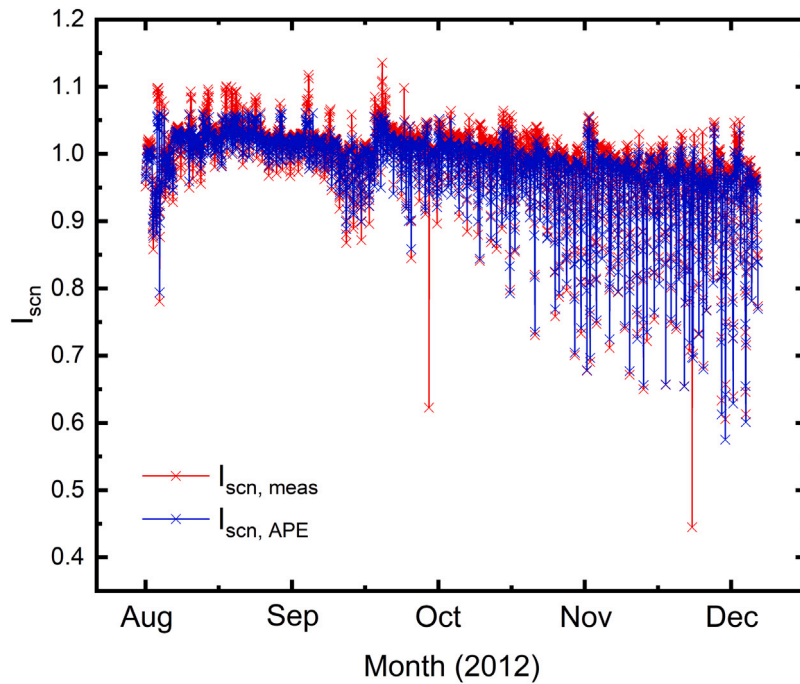
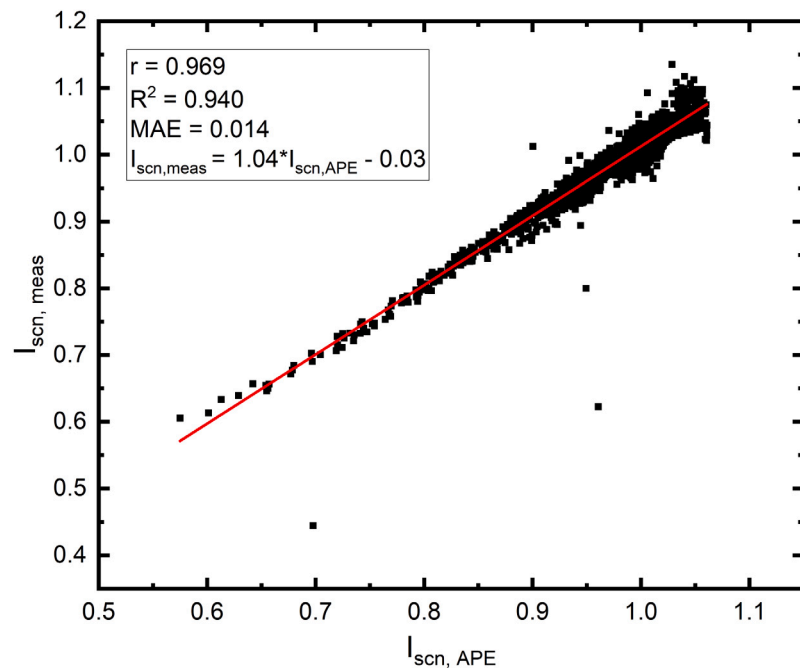**Fig. 6.** Time series validation of $f(\varphi)$ for August 2012–December 2012.

Fig. 7. Validation of $f(\varphi)$ for August 2012–December 2012.

4.2.1. Existing functions: Air mass and clearness index

The AM_a and AM_a-K_t spectral correction functions have been derived from the same NREL data used to derive $f(\varphi)$. The derived functions are presented in Figs. 8 and 9. AM_a values are calculated using the method proposed in [58]. Atmospheric pressure was measured on site and the solar position parameters, namely the zenith and azimuth angles, were calculated using the solar position algorithm [59]. K_t values were calculated according to:

$$K_t = \frac{GHI}{GEI}, \tag{7}$$

where GHI is the global horizontal irradiance as measured by a Kipp and Zonen CM22 pyranometer, and GEI is the global extraterrestrial radiation calculated by [60]:

$$GEI = \frac{S}{\mathbf{R}^2} \times \cos Z, \tag{8}$$

where the S is the solar constant, equal to 1367 W m^{-2}, $\mathbf{R}$ is the Earth radius vector, and Z is the solar zenith angle calculated using the solar position algorithm cited earlier. A higher K_t value indicates clear skies, whereas a lower value indicates cloudier skies. Typically, a K_t of 0.8 is indicative of almost completely clear skies [61]. It is important to note that in the original publication of the AM_a-K_t function [14]
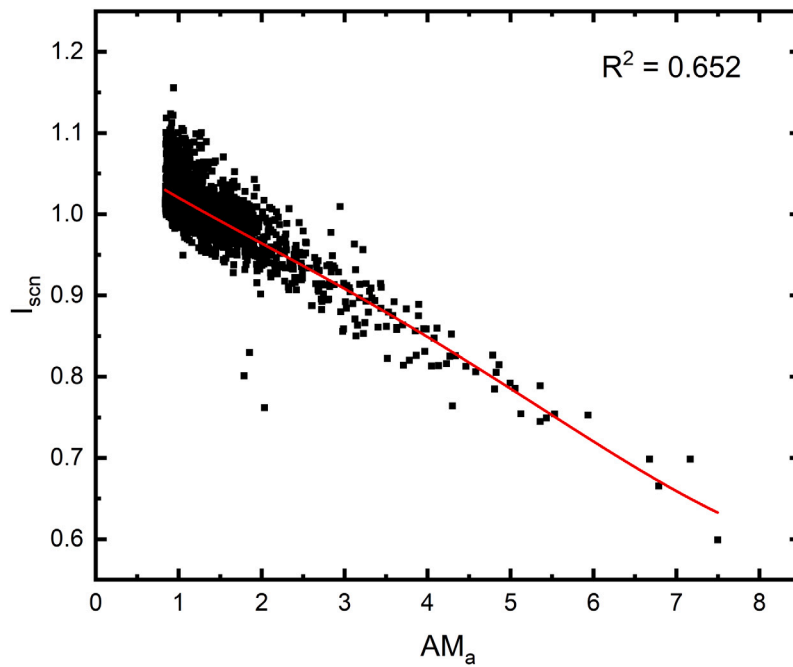
Fig. 8. $f(\text{AM}_a)$ for January 2013–August 2013.

the authors correlated AM_a and K_t with UF, whereas in this study a new correlation is derived with respect to I_{scn}. This modification is made to enable a more direct comparison between the accuracy of the different functions. I_{scn} can offer a more intuitive way of understanding PV spectral performance without the need for complex device-specific measurements of spectral response.

4.2.2. Comparison of model fits

There is a much weaker relationship between AM_a and I_{scn}, evidenced by an R^2 value of only 0.652 in Fig. 8, compared to 0.870 for the APE function shown in Fig. 5. Although the AM_a-K_t function in Fig. 9 offers a better fit to I_{scn} than AM_a alone, the final R^2 value of 0.828 still falls short of that achieved by $f(\varphi)$. Although the difference relative to $f(\varphi)$ is smaller, it is notable that the single variable APE function is still able to outperform the more complex multivariable AM_a-K_t function.

The following section compares how the fitting accuracy of the different spectral correction models translates into predictive accuracy of PV performance.

4.2.3. Comparison of predictive accuracy

The correlations between the predicted and calculated values of I_{scn} using both $f(\text{AM}_a)$ and $f(\text{AM}_a, \text{K}_t)$ are plotted in Figs. 10 and 11, respectively.

The weakness of the $\text{AM}_a - I_{scn}$ correlation in Fig. 8 translates into a weaker predictive power of the AM_a function in Fig. 10. The AM_a-K_t function offers a more reliable prediction of I_{scn} than the AM_a function, evident from the reduced spread in data, but there is still significant variability in the prediction when compared to the spread of data in the APE function in Fig. 5. The R^2 analysis shows that although there is only a 5% improvement in the initial model for the APE function compared to the AM_a-K_t function, this slight improvement translates into a disproportionately greater improvement in prediction accuracy of almost 15%. This shows the ability of the APE function to incorporate not only the effects of cloud cover and air mass on the spectrum, and therefore PV performance, but also additional effects from other atmospheric parameters. A comparison of all of the fit statistics for each of the functions is presented in Table 2.

Table 2
Fit statistics for the AM_a, AM_a-K_t, and APE spectral correction functions absolute predictive accuracy test.

Correlation	Statistic		
	r	R^2	MAE
$I_{scn,meas}(\text{AM}_a)$	0.874	0.765	0.024
$I_{scn,meas}(\text{AM}_a, \text{K}_t)$	0.898	0.806	0.022
$I_{scn,meas}(\varphi)$	0.969	0.940	0.014

Table 3
Degree of matching between the measured and predicted values of I_{scn} for each of the proposed APE function and two traditional functions, $f(\text{AM}_a)$ and $f(\text{AM}_a, \text{K}_t)$.

	SCF		
	$f(\text{AM}_a)$	$f(\text{AM}_a, \text{K}_t)$	$f(\varphi)$
Matching (%)	77	81	94

In terms of the time series analysis, the measured and calculated normalised short-circuit currents are plotted against time for $f(\text{AM}_a)$ and $f(\text{AM}_a, \text{K}_t)$ in Figs. 12 and 13, respectively. The time series analysis shows that all three functions are capable of capturing the overall seasonal trend in I_{scn} from August to December, where I_{scn} exhibits a continual decrease in magnitude and increase in variability. However, $f(\varphi)$ has a significantly greater predictive accuracy, compared to $f(\text{AM}_a)$ and $f(\text{AM}_a, \text{K}_t)$, across the full duration of the investigation. The degree of matching between each of the three SCFs is summarised quantitatively in Table 3.

Deviations of the predicted from the measured values for all three functions tend to be underestimates, which was expected following the gradients generated in the absolute predictive accuracy analysis being > 1. However, the deviations in the case of $f(\text{AM}_a)$ are visibly greater than those for $f(\varphi)$. Furthermore, the temporal resolution at which $f(\varphi)$ is able to capture the variations in I_{scn} is far beyond that of $f(\text{AM}_a)$. The ability of $f(\varphi)$ to model fluctuations at a 15-min time resolution, which is the limit of the measured data in this study, means that the applicability of the function is greatly enhanced. The reason for this improved modelling at shorter time intervals is down to the APE's higher sensitivity to changes in the spectrum. Changes in air
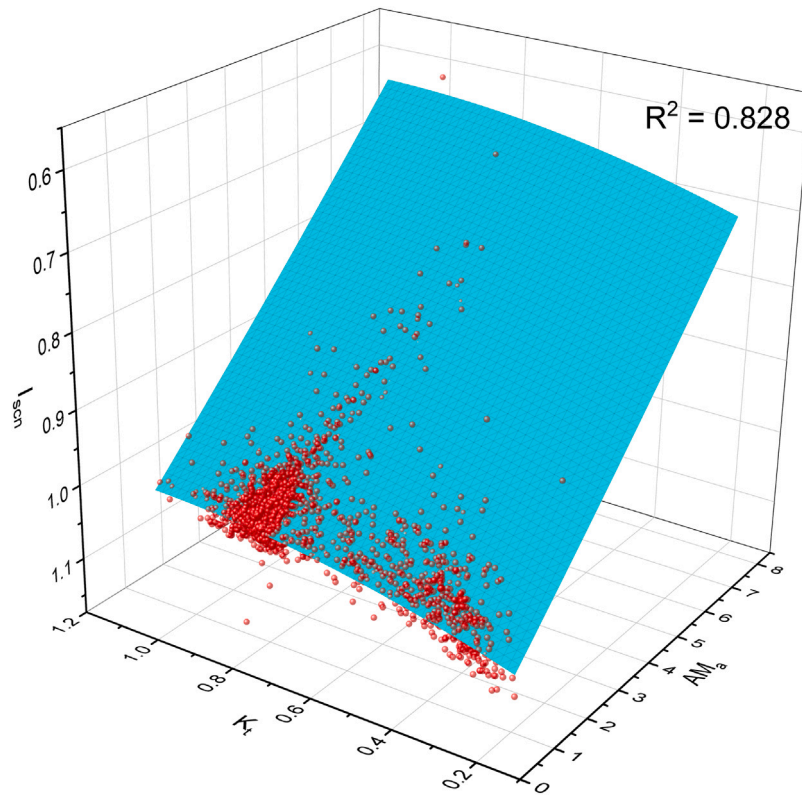
Fig. 9. $f(\mathrm{AM}_a, \mathrm{K}_t)$ for January 2013–August 2013.
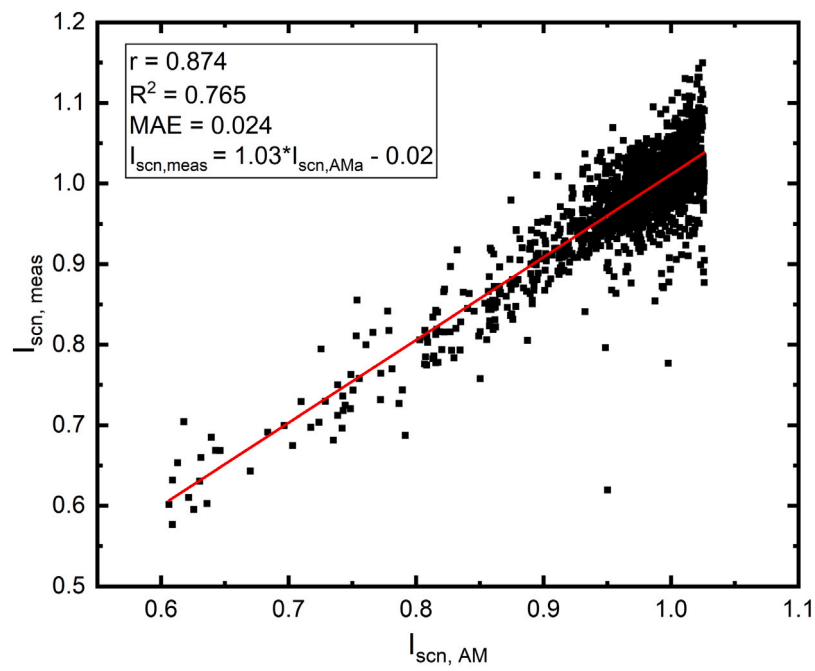
Fig. 10. Validation of $f(\mathrm{AM}_a)$ for August 2012–December 2012.
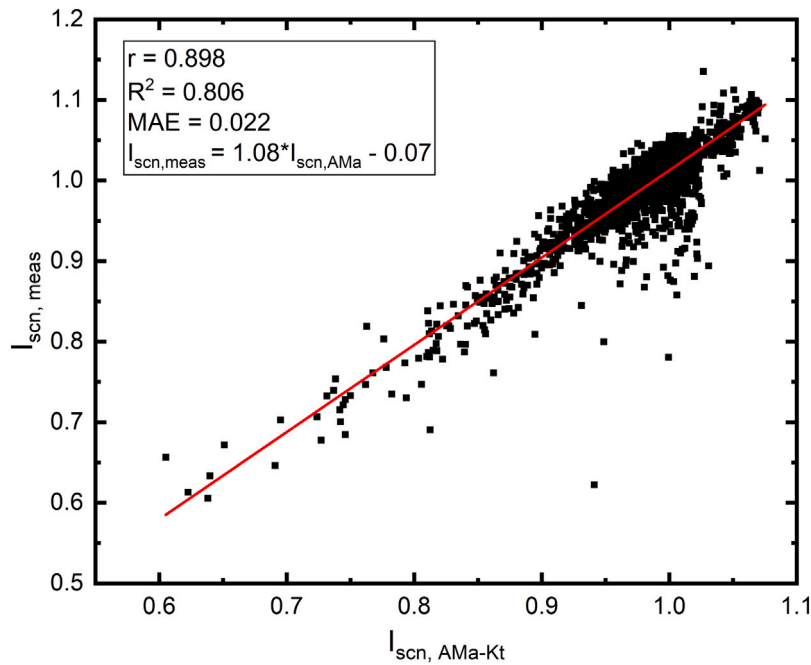
Fig. 11. Validation of $f(\mathrm{AM}_a, \mathrm{K}_t)$ for August 2012–December 2012.
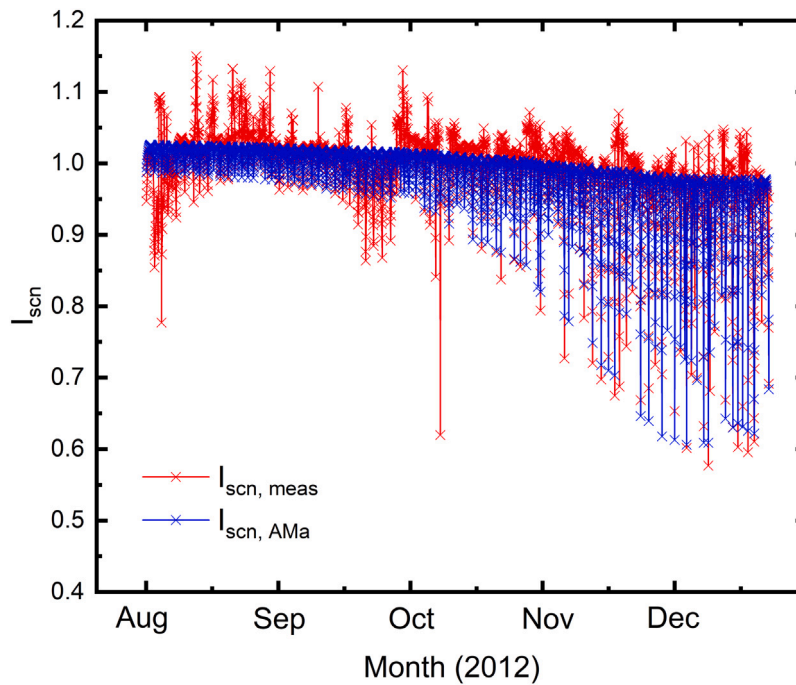

Fig. 12. Time series validation of $f(\mathrm{AM}_a)$ for August 2012–December 2012.

mass are driven only by the sun's position in the sky, which changes slowly, therefore high frequency changes in the spectrum resulting from high frequency changes in the sky conditions and atmospheric composition cannot be captured by using changes in the air mass as a proxy. Furthermore, an APE value can be derived from a spectrum, measured at any time, almost instantaneously.

This point regarding the temporal resolution at which the different functions can capture changes in the spectrum also relates to the fact that although $f(\mathrm{AM}_a)$ and $f(\mathrm{AM}_a, \mathrm{K}_t)$ are able to capture situations where $I_{scn} < 1$ in the winter months, they are incapable of doing so in the summer months. This is in contrast to $f(\varphi)$, which captures both $I_{scn} < 1$ and $I_{scn} > 1$ throughout the year. The reason for

this difference lies in the factors affecting the spectrum in different months. The shift in I_{scn} to lower values over the course of the year is primarily a result of the changing solar elevation, which is lower in winter months. Therefore, air mass exhibits a dominant role in the long-term seasonal variation in the spectrum, hence AM_a-based models are capable of accurately modelling this variation. On the other hand, high frequency dips in I_{scn} in the summer months are not driven by changes in air mass, but rather atmospheric composition. For example, changes in cloud cover patterns, atmospheric turbidities, and the distributions of different gases such as ozone and sulphur dioxide. Therefore, instantaneous characterisation of the spectrum to determine
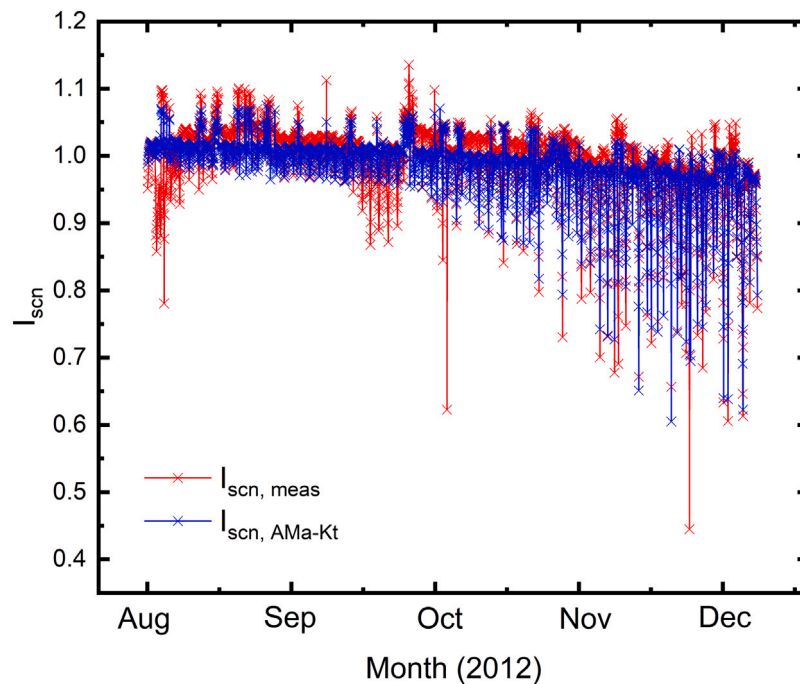
Fig. 13. Time series validation of $f(\mathrm{AM}_a, \mathrm{K}_t)$ for August 2012–December 2012.

the spectral influence on PV performance, using $f(\varphi)$, is more accurate both in the short and long term.

In terms of how each individual function compares to the others for different ranges of I_{scn}, it can be seen that $f(\mathrm{AM}_a, \mathrm{K}_t)$ offers an improved prediction compared to $f(\mathrm{AM}_a)$, in particular in terms of its ability to predict I_{scn} values greater than 1. This is as expected for aSi modules since such modules tend to operate more efficiently in cloudier conditions, the effects of which are modelled more accurately in $f(\mathrm{AM}_a, \mathrm{K}_t)$ than $f(\mathrm{AM}_a)$ due to the inclusion of the clearness index parameter. However, $f(\varphi)$ still outperforms $f(\mathrm{AM}_a, \mathrm{K}_t)$, generating either a similar or better forecast of I_{scn}. The most notable improvements that are achieved by $f(\varphi)$ over $f(\mathrm{AM}_a, \mathrm{K}_t)$ are for I_{scn} values less than 1. This indicates that although K_t can improve the prediction accuracy of $f(\mathrm{AM}_a)$ by incorporating the effects of cloud cover, hence for $I_{scn} > 1$, the APE function is able to account not only for the effects of air mass and cloud cover, but also the effects of other parameters omitted by the $\mathrm{AM}_a - \mathrm{K}_t$ function, which also impact the spectrum.

Finally, whether the high predictive accuracy of $f(APE)$ is maintained for other PV technologies is yet to be tested. Questions have been raised in the literature about the uncertainty in the relationship between the APE and the spectrum, in particular at longer wavelengths [62]. Therefore, it is necessary to validate the proposed methodology for other PV technologies, in particular those with a wider spectral response range than aSi. Crystalline silicon (c-Si) PV would be a good starting point as this technology maintains a response at longer wavelengths than aSi. In addition, c-Si has dominated the PV market in recent years, in particular for residential rooftop applications [63,64].

5. Analysis summary

The proposed methodology for analysing the spectral influence on PV performance has been used to derive an APE spectral correction function from eight months of empirical data measured in Golden, Colorado. The derived function has been validated using the remaining four months of data from the year to compare the predicted and calculated values of I_{scn}, and to compare its performance to that of the traditional air mass model and a modified air mass model that includes the effects of cloud cover. Up to 30% absolute percentage

improvement in predictive accuracy can be achieved through the use of the derived APE function, which improves on traditional models both in terms of absolute prediction accuracy and the temporal resolution at which accurate predictions are achieved. These improvements have been quantified using a range of statistical parameters, namely the Pearson's correlation coefficient (r), coefficient of determination (R^2), and the mean absolute error (MAE). In all statistical tests, the APE function outperforms the air mass-based functions by a significant margin.

6. Conclusion

PV performance modelling is essential for the success of PV systems. Traditional approaches to account for the spectral influence on PV performance and predictions thereof have been dominated by the use of proxy variables, in particular the air mass parameter. The majority of such functions suffer from increased uncertainty due to their limited scope of inclusion of factors that affect the solar spectral distribution.

The APE is shown in this study to be a single parameter capable of accurately characterising spectral distributions for effective use in computing the effect of the spectrum on PV performance. The spectral correction methodology presented in this study, which is validated using an aSi PV module deployed in Golden, Colorado, shows significant improvements in prediction accuracy and forecasting time resolution when compared to two air mass-based approaches. The greatest improvement is found with respect to $f(\mathrm{AM}_a)$, but even after the inclusion of the clearness index in $f(\mathrm{AM}_a)$ to account for the spectral effects of cloud cover, $f(\varphi)$ still more accurately models I_{scn} for values both greater than and less than unity.

Improvements in accuracy achieved by $f(\varphi)$, compared with $f(\mathrm{AM}_a)$ and $f(\mathrm{AM}_a, \mathrm{K}_t)$, reach up to 30% considering the statistical ability to explain variations in PV output due to variations in the incident solar spectrum. The coefficients for $f(\varphi)$ for the aSi module are presented so that the function may easily be integrated into any PV performance model to improve modelling accuracy.

Although aSi performance is most susceptible to spectral changes, further work is still required to validate the proposed methodology for a range of PV technologies. Finally, validation of the model in different climatic regions is necessary to test the worldwide generalisability of the proposed methodology.

CRediT authorship contribution statement

Rajiv Daxini: Conceptualization, Methodology, Software, Validation, Formal analysis, Writing – original draft, Writing – review & editing, Visualization. **Yanyi Sun:** Writing – review & editing. **Robin Wilson:** Writing – review & editing, Supervision. **Yupeng Wu:** Writing – review & editing, Supervision.

Declaration of competing interest

The authors declare that they have no known competing financial interests or personal relationships that could have appeared to influence the work reported in this paper.

Data availability

The data used in this manuscript are available from http://dx.doi.org/10.5439/1052221 and http://dx.doi.org/10.21948/1811521

Acknowledgements

References

[1] W. Palz, Solar Power for the World: What You Wanted to Know About Photovoltaics, Vol. 4, CRC Press, 2013.

[2] T. Ma, H. Yang, L. Lu, Solar photovoltaic system modeling and performance prediction, Renew. Sustain. Energy Rev. 36 (2014) 304–315.

[3] A. Mellit, A.M. Pavan, V. Lughi, Deep learning neural networks for short-term photovoltaic power forecasting, Renew. Energy 172 (2021) 276–288.

[4] D. Koster, F. Minette, C. Braun, O. O'Nagy, Short-term and regionalized photovoltaic power forecasting, enhanced by reference systems, on the example of Luxembourg, Renew. Energy 132 (2019) 455–470.

[5] L. Ryan, J. Dillon, S. La Monaca, J. Byrne, M. O'Malley, Assessing the system and investor value of utility-scale solar PV, Renew. Sustain. Energy Rev. 64 (2016) 506–517.

[6] B. Espinar, J.-L. Aznarte, R. Girard, A.M. Moussa, G. Kariniotakis, et al., Photovoltaic forecasting: A state of the art, in: Proceedings 5th European PV-Hybrid and Mini-Grid Conference, Citeseer, 2010, pp. 250–255.

[7] A.T. Eseye, J. Zhang, D. Zheng, Short-term photovoltaic solar power forecasting using a hybrid wavelet-PSO-SVM model based on SCADA and meteorological information, Renew. Energy 118 (2018) 357–367.

[8] M. Kerr, A. Cuevas, Generalized analysis of the illumination intensity vs. open-circuit voltage of solar cells, Sol. Energy 76 (1–3) (2004) 263–267.

[9] B.V. Chikate, Y. Sadaware, B. Sewagram, The factors affecting the performance of solar cell, Int. J. Comput. Appl. 1 (1) (2015) 0975–8887.

[10] K. Vidyanandan, An overview of factors affecting the performance of solar PV systems, Energy Scan 27 (28) (2017) 216.

[11] S. Nann, K. Emery, Spectral effects on PV-device rating, Sol. Energy Mater. Sol. Cells 27 (3) (1992) 189–216.

[12] N. Chivelet, Analysis of spectral factor of different commercial PV modules based on measured data, in: 14 Th European PV Conference, 1997, pp. 282–283.

[13] R. Rüther, G. Kleiss, K. Reiche, Spectral effects on amorphous silicon solar module fill factors, Sol. Energy Mater. Sol. Cells 71 (3) (2002) 375–385.

[14] R. Gottschalg, T. Betts, D. Infield, M. Kearney, On the importance of considering the incident spectrum when measuring the outdoor performance of amorphous silicon photovoltaic devices, Meas. Sci. Technol. 15 (2) (2004) 460.

[15] N. Lindsay, Q. Libois, J. Badosa, A. Migan-Dubois, V. Bourdin, Errors in PV power modelling due to the lack of spectral and angular details of solar irradiance inputs, Sol. Energy 197 (2020) 266–278.

[16] Y. Hirata, T. Tani, Output variation of photovoltaic modules with environmental factors—I. The effect of spectral solar radiation on photovoltaic module output, Sol. Energy 55 (6) (1995) 463–468.

[17] R. Gottschalg, T.R. Betts, D. Infield, M.J. Kearney, Experimental investigation of spectral effects on amorphous silicon solar cells in outdoor operation, in: Conference Record of the Twenty-Ninth IEEE Photovoltaic Specialists Conference, 2002, IEEE, 2002, pp. 1138–1141.

[18] T. Minemoto, M. Toda, S. Nagae, M. Gotoh, A. Nakajima, K. Yamamoto, H. Takakura, Y. Hamakawa, Effect of spectral irradiance distribution on the outdoor performance of amorphous Si//thin-film crystalline Si stacked photovoltaic modules, Sol. Energy Mater. Sol. Cells 91 (2–3) (2007) 120–122.

[19] D.L. King, Photovoltaic module and array performance characterization methods for all system operating conditions, in: AIP Conference Proceedings. Vol. 394, American Institute of Physics, 1997, pp. 347–368.

[20] S. Nann, C. Riordan, Solar spectral irradiance under overcast skies (solar cell performance effects), in: IEEE Conference on Photovoltaic Specialists, IEEE, 1990, pp. 1110–1115.

[21] T. Ishii, K. Otani, T. Takashima, Y. Xue, Solar spectral influence on the performance of photovoltaic (PV) modules under fine weather and cloudy weather conditions, Prog. Photovolt., Res. Appl. 21 (4) (2013) 481–489.

[22] M. Simon, E.L. Meyer, The effects of spectral evaluation of c-Si modules, Prog. Photovolt., Res. Appl. 19 (1) (2011) 1–10.

[23] A.F. Bais, C.S. Zerefos, C. Meleti, I.C. Ziomas, K. Tourpali, Spectral measurements of solar UVB radiation and its relations to total ozone, SO2, and clouds, J. Geophys. Res.: Atmos. 98 (D3) (1993) 5199–5204.

[24] S. Nann, C. Riordan, Solar spectral irradiance under clear and cloudy skies: Measurements and a semiempirical model, J. Appl. Meteorol. 30 (4) (1991) 447–462.

[25] J.S. Bartlett, Á.M. Ciotti, R.F. Davis, J.J. Cullen, The spectral effects of clouds on solar irradiance, J. Geophys. Res.: Oceans 103 (C13) (1998) 31017–31031.

[26] K.A. Klise, C.W. Hansen, J.S. Stein, Dependence on geographic location of air mass modifiers for photovoltaic module performance models, in: 2015 IEEE 42nd Photovoltaic Specialist Conference, PVSC, IEEE, 2015, pp. 1–5.

[27] L. Nelson, M. Frichtl, A. Panchula, Changes in cadmium telluride photovoltaic system performance due to spectrum, IEEE J. Photovolt. 3 (1) (2012) 488–493.

[28] M. Lee, A. Panchula, Spectral correction for photovoltaic module performance based on air mass and precipitable water, in: 2016 IEEE 43rd Photovoltaic Specialists Conference, PVSC, IEEE, 2016, pp. 1351–1356.

[29] B.C. Duck, C.J. Fell, Improving the spectral correction function, in: 2016 IEEE 43rd Photovoltaic Specialists Conference, PVSC, IEEE, 2016, pp. 2647–2652.

[30] C. Gueymard, et al., SMARTS2: A Simple Model of the Atmospheric Radiative Transfer of Sunshine: Algorithms and Performance Assessment, Florida Solar Energy Center Cocoa, FL, 1995.

[31] B.C. Duck, C.J. Fell, Comparison of methods for estimating the impact of spectrum on PV output, in: 2015 IEEE 42nd Photovoltaic Specialist Conference, PVSC, IEEE, 2015, pp. 1–6.

[32] J. Chantana, Y. Imai, Y. Kawano, Y. Hishikawa, K. Nishioka, T. Minemoto, Impact of average photon energy on spectral gain and loss of various-type PV technologies at different locations, Renew. Energy 145 (2020) 1317–1324.

[33] M. Tsuji, J. Chantana, K. Nakayama, Y. Kawano, Y. Hishikawa, T. Minemoto, Utilization of spectral mismatch correction factor for estimation of precise outdoor performance under different average photon energies, Renew. Energy 157 (2020) 173–181.

[34] V. Tatsiankou, K. Hinzer, J. Mohammed, A. Muron, M. Wilkins, J. Haysom, H. Schriemer, S. Myrskog, Reconstruction of solar spectral resource using limited spectral sampling for concentrating photovoltaic systems, in: Photonics North 2013. Vol. 8915, International Society for Optics and Photonics, 2014, 891506.

[35] V. Tatsiankou, K. Hinzer, H. Schriemer, S. Kazadzis, N. Kouremeti, J. Gröbner, R. Beal, Extensive validation of solar spectral irradiance meters at the world radiation center, Sol. Energy 166 (2018) 80–89.

[36] C. Cornaro, A. Andreotti, Influence of average photon energy index on solar irradiance characteristics and outdoor performance of photovoltaic modules, Prog. Photovolt., Res. Appl. 21 (5) (2013) 996–1003.

[37] R. Moreno-Sáez, L. Mora-López, Modelling the distribution of solar spectral irradiance using data mining techniques, Environ. Model. Softw. 53 (2014) 163–172.

[38] T. Rodziewicz, M. Rajfur, Numerical procedures and their practical application in PV modules' analyses. Part II: Useful fractions and APE, Opto-Electron. Rev. 27 (2) (2019) 149–160.

[39] M. Piliougine, D. Elizondo, L. Mora-López, M. Sidrach-de Cardona, Multilayer perceptron applied to the estimation of the influence of the solar spectral distribution on thin-film photovoltaic modules, Appl. Energy 112 (2013) 610–617.

[40] L.A. Neves, G.C. Leite, R.C. MacKenzie, R.A. Ferreira, M.P. Porto, A methodology to simulate solar cells electrical response using optical-electrical mathematical models and real solar spectra, Renew. Energy 164 (2021) 968–977.

[41] C.N. Jardine, T. Betts, R. Gottschalg, D. Infield, K. Lane, Influence of spectral effects on the performance of multijunction amorphous silicon cells, in: Proc. Photovoltaic in Europe Conference, 2002, pp. 1756–1759.

[42] G. Nofuentes, B. García-Domingo, J. Muñoz, F. Chenlo, Analysis of the dependence of the spectral factor of some PV technologies on the solar spectrum distribution, Appl. Energy 113 (2014) 302–309.

[43] S.R. Williams, T.R. Betts, T. Helf, R. Gottschalg, H. Beyer, D. Infield, Modelling long-term module performance based on realistic reporting conditions with consideration to spectral effects, in: 3rd World Conference On Photovoltaic Energy Conversion, 2003. Proceedings of. Vol. 2, IEEE, 2003, pp. 1908–1911.

[44] T. Minemoto, S. Fukushige, H. Takakura, Difference in the outdoor performance of bulk and thin-film silicon-based photovoltaic modules, Sol. Energy Mater. Sol. Cells 93 (6–7) (2009) 1062–1065.

[45] IEC, Photovoltaic Devices: Solar Simulator Performance Requirements, IEC 60904-9, IEC Central Office Geneva, 2007.

[46] T. Minemoto, Y. Nakada, H. Takahashi, H. Takakura, Uniqueness verification of solar spectrum index of average photon energy for evaluating outdoor performance of photovoltaic modules, Sol. Energy 83 (8) (2009) 1294–1299.

[47] T. Minemoto, S. Nagae, H. Takakura, Impact of spectral irradiance distribution and temperature on the outdoor performance of amorphous Si photovoltaic modules, Sol. Energy Mater. Sol. Cells 91 (10) (2007) 919–923.

[48] S. Nagae, M. Toda, T. Minemoto, H. Takakura, Y. Hamakawa, Evaluation of the impact of solar spectrum and temperature variations on output power of silicon-based photovoltaic modules, Sol. Energy Mater. Sol. Cells 90 (20) (2006) 3568–3575.

[49] T. Ishii, K. Otani, T. Takashima, Effects of solar spectrum and module temperature on outdoor performance of photovoltaic modules in round-robin measurements in Japan, Prog. Photovolt., Res. Appl. 19 (2) (2011) 141–148.

[50] B.H. King, C.W. Hansen, D. Riley, C.D. Robinson, L. Pratt, Procedure to Determine Coefficients for the Sandia Array Performance Model (SAPM), Tech. rep., Sandia National Lab.(SNL-NM), Albuquerque, NM (United States), 2016.

[51] D.L. King, J.A. Kratochvil, W.E. Boyson, Photovoltaic Array Performance Model, United States. Department of Energy, 2004.

[52] W. Marion, A. Anderberg, C. Deline, S. Glick, M. Muller, G. Perrin, J. Rodriguez, S. Rummel, K. Terwilliger, T. Silverman, User's Manual for Data for Validating Models for PV Module Performance, Tech. rep., National Renewable Energy Lab (NREL), Golden, CO (United States), 2014.

[53] T. Stoffel, A. Andreas, NREL Solar Radiation Research Laboratory (SRRL): Baseline Measurement System (BMS); Golden, Colorado (Data), Tech. rep., National Renewable Energy Lab (NREL), Golden, CO (United States), 1981.

[54] L.V. Mercaldo, M.L. Addonizio, M. Della Noce, P.D. Veneri, A. Scognamiglio, C. Privato, Thin film silicon photovoltaics: Architectural perspectives and technological issues, Appl. Energy 86 (10) (2009) 1836–1844.

[55] E.H. Rusnindyo, E.A. Karuniawan, A.A. Setiawan, F.D. Wijaya, Building integrated thin film photovoltaic performance modelling on conventional building, in: AIP Conference Proceedings. Vol. 2255, AIP Publishing LLC, 2020, 070023.

[56] M. Piliougine, P. Sánchez-Friera, G. Petrone, F.J. Sánchez-Pacheco, G. Spagnuolo, M. Sidrach-de Cardona, New model to study the outdoor degradation of thin–film photovoltaic modules, Renew. Energy (2022).

[57] I. Hughes, T. Hase, Measurements and their Uncertainties: A Practical Guide to Modern Error Analysis, OUP Oxford, 2010.

[58] F. Kasten, A.T. Young, Revised optical air mass tables and approximation formula, Appl. Opt. 28 (22) (1989) 4735–4738.

[59] I. Reda, A. Andreas, Solar position algorithm for solar radiation applications, Sol. Energy 76 (5) (2004) 577–589.

[60] M. Iqbal, An Introduction to Solar Radiation, Elsevier, 2012.

[61] P. Tzoumanikas, E. Nikitidou, A. Bais, A. Kazantzidis, The effect of clouds on surface solar irradiance, based on data from an all-sky imaging system, Renew. Energy 95 (2016) 314–322.

[62] G. Nofuentes, C. Gueymard, J. Aguilera, M. Pérez-Godoy, F. Charte, Is the average photon energy a unique characteristic of the spectral distribution of global irradiance? Sol. Energy 149 (2017) 32–43.

[63] Y. Yang, A. Yu, B. Hsu, W. Hsu, A. Yang, C. Lan, Development of high-performance multicrystalline silicon for photovoltaic industry, Prog. Photovolt., Res. Appl. 23 (3) (2015) 340–351.

[64] M.E. Meral, F. Dincer, A review of the factors affecting operation and efficiency of photovoltaic based electricity generation systems, Renew. Sustain. Energy Rev. 15 (5) (2011) 2176–2184.